Precambrian Research 305 (2018) 295–309

Contents lists available at ScienceDirect

Precambrian Research

journal homepage: www.elsevier.com/locate/precamres

Paleomagnetism and rock magnetism of the ca. 1.87 Ga Pearson Formation, Northwest Territories, Canada: A test of vertical-axis rotation within the Great Slave basin

Zheng Gong[a,*], XinXin Xu[a], David A.D. Evans[a], Paul F. Hoffman[b,c], Ross N. Mitchell[d], Wouter Bleeker[e]

[a] Department of Geology and Geophysics, Yale University, 210 Whitney Avenue, New Haven, CT 06511, USA
[b] Department of Earth and Planetary Sciences, Harvard University, 20 Oxford Street, Cambridge, MA 02138, USA
[c] School of Earth and Ocean Sciences, University of Victoria, PO Box 1700, Victoria, BC V8W 2Y2, Canada
[d] Earth Dynamics Research Group, The Institute for Geoscience Research (TIGeR), Department of Applied Geology, Curtin University, GPO Box U1987, WA 6845, Australia
[e] Geological Survey of Canada, 601 Booth Street, Ottawa, ON K1S 0E8, Canada

ARTICLE INFO

Keywords:
Slave craton
Coronation APWP
Vertical-axis rotation
Pearson Formation
Paleomagnetism
Rock magnetism
Paleoproterozoic

ABSTRACT

A geometrically quantitative plate-kinematic model, based on paleomagnetism, for the initial assembly of Laurentia has taken form in the past few decades. Within this framework, there remains but one problematic interval of data predominantly from the Slave craton, which is the 1.96–1.87 Ga Coronation apparent polar wander path (APWP). The Coronation APWP shows large (~110°) back-and-forth oscillations that are difficult to explain in terms of plate motion. Nonetheless, poles from the Coronation APWP have been incorporated in various paleogeographic reconstructions of Laurentia and the supercontinent Nuna, pointing to the importance of testing its veracity. In this study, we conducted a detailed paleomagnetic and rock magnetic study of the ca. 1.87 Ga Pearson Formation, East Arm of Great Slave Lake, Northwest Territories, Canada. Our results show that Pearson Formation yields a characteristic remanent magnetization carried by single-domain or small pseudo-single-domain magnetite. The age of the magnetization is constrained to be older than Paleoproterozoic deformation and is interpreted as primary. Paleomagnetic declinations reveal a one-to-one correlation with local structural attitudes, indicating that some small blocks in the fold belt likely experienced significant (~60°) vertical-axis rotations, presumably related to large dextral displacements along the McDonald Fault system. Alternative explanations, such as true polar wander or a non-dipole magnetic field, are considered less parsimonious for the data presented here. It is suspected that some existing Christie Bay Group poles (the Stark and Tochatwi Formations), which were sampled in areas with anomalous structural attitudes and differ from time-equivalent poles obtained from areas of the Slave craton far from major transcurrent faults, may similarly suffer from vertical-axis rotation. We suggest further study before using possibly rotated Christie Bay Group poles for paleogeographic reconstructions.

1. Introduction

Laurentia owes its existence to the amalgamation of six Archean cratons in early Proterozoic time (2.0–1.7 Ga; Hoffman, 1988a, 2014). The pre- and syn-collisional kinematic histories of these cratons are crucial for testing the current reconstruction models of Laurentia, and in a larger perspective, the assembly of the supercontinent Nuna. Apparent polar wander paths (APWPs) of these Archean cratons have been constructed and compared in an attempt to quantify changes of their relative orientations and positions during the amalgamation (Mitchell et al., 2014; Buchan et al., 2016; Kilian et al., 2016), but controversies remain owing to the sparsity of well-defined paleomagnetic poles.

The Slave craton, one of the key components of Laurentia, plays an important role in the amalgamation of Laurentia by its collision with the Rae craton at 1.97 Ga and the Hottah terrane at 1.88 Ga (Fig. 1a; Hoffman, 1988a, 2014; Bowring and Grotzinger, 1992). The APWP of the Slave craton in the critical 1.96–1.87 Ga interval was constructed mainly based on studies in the 1970's, and was interpreted as a long loop, termed the "Coronation loop" (McGlynn and Irving, 1978). Since then, more paleomagnetic poles of 1.96–1.87 Ga age have been

* Corresponding author.
E-mail address: z.gong@yale.edu (Z. Gong).

https://doi.org/10.1016/j.precamres.2017.11.021
Received 29 August 2017; Received in revised form 21 November 2017; Accepted 27 November 2017
Available online 28 November 2017
0301-9268/

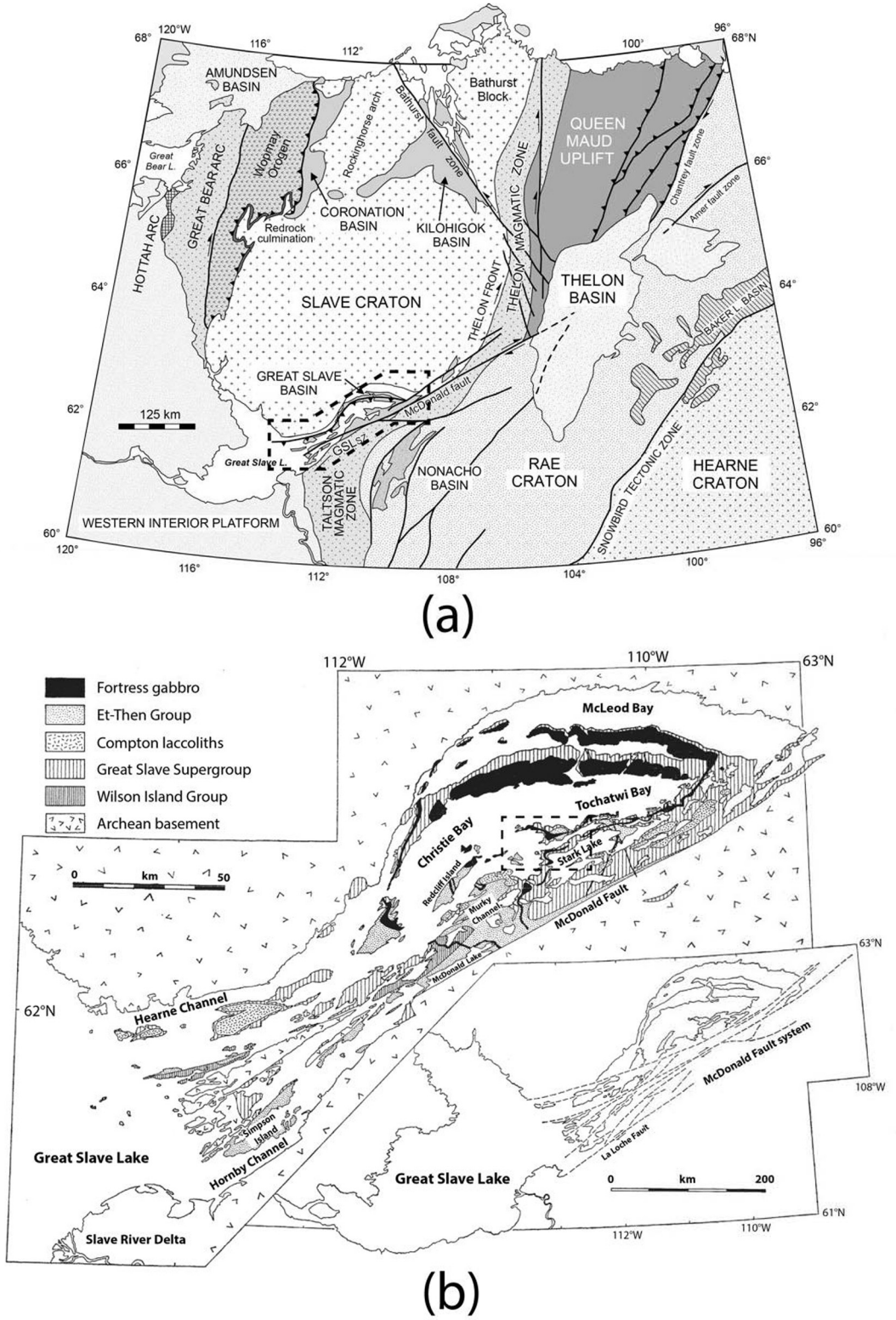

Fig. 1. (a) Tectonic map of the Slave craton and environs (Hoffman, 1989; Helmstaedt, 2009). Dashed box indicates the area depicted in Fig. 1b. (b) Geologic map of the East Arm of Great Slave Lake (Hoffman, 1973). Dashed box indicates the area shown in Fig. 5.

obtained, which collectively show a series of back-and-forth oscillations along a large arc (> 110°; Fig. 2; Table 1). In this work, we use Coronation APWP to refer to the oscillatory paleomagnetic poles of the Slave craton at 1.96–1.87 Ga. If the Coronation APWP represents the actual paleogeographic evolution of the Slave craton in Paleoproterozoic time, then the implied motions are unusual in their oscillatory style.

Hypotheses other than plate motion have been invoked to explain the Coronation APWP. One hypothesis attributes the Coronation APWP to local vertical-axis rotation of the sampling areas, which was initially proposed by Bingham and Evans (1976) and then further developed by Irving et al. (2004). They suspected that some sampling areas in the

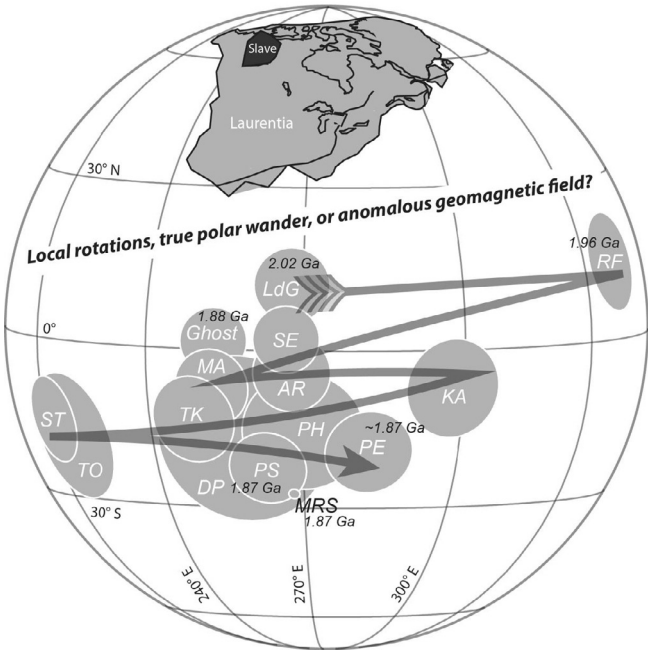

Fig. 2. Stereographic projection of the Coronation APWP. Paleomagnetic poles are summarized in Table 1. In ascending stratigraphic order: LdG, Lac de Gras dykes; RF, Rifle Formation; Ghost, Ghost dykes; MA, Mara Formation; AR, Akaitcho River Formation; SE, Seton Formation; PH, Peacock Hills Formation; KA, Kahochella Group; DP, Douglas Peninsular Formation; ST, Stark Formation; TO, Tochatwi Formation; TK, Takiyuak Formation; PS, Peninsular sill; MRS, Mara River sills; PE, Pearson Formation.

Great Slave and Kilohigok basins may have experienced vertical-axis rotations due to the shearing produced by the conjugate McDonald and Bathurst Fault systems, respectively, as commonly observed in strike-slip tectonic settings (e.g., Kamerling and Luyendyk, 1979; Hornafius et al., 1986). Therefore, the Coronation APWP could be a result of these local rotations (Irving et al., 2004). Mitchell et al. (2010) applied trans-cratonic structural corrections on individual Coronation poles and argued that these poles were affected by at most minor amounts (~12°) of vertical-axis rotation. Instead, Mitchell et al. (2010) suggested that the majority of variance among Coronation poles could result from true polar wander, whereby the entire solid Earth rotates with respect to its spin axis in order to adjust to the evolving mantle mass heterogeneities.

Definitively testing the vertical-axis rotation hypothesis for the Coronation APWP requires adequate consideration of structural complexities on local scales and on a case-by-case basis. We approach this test by conducting a detailed paleomagnetic and rock magnetic study of the ca. 1.87 Ga Pearson Formation (basalt) in the Great Slave basin, East Arm of Great Slave Lake, Northwest Territories, Canada. We sampled the basal Pearson Formation from areas with different structural attitudes, where the Pearson basalts conformably overlie the Portage Inlet Formation (evaporitic siltstone). Therefore, Pearson samples from different areas should be broadly similar in age because of their comparable stratigraphic levels within a lateral distance of ~20 km. If the local structural anomalies do result from rotations within the right-lateral McDonald Fault system, the paleomagnetic directions gleaned from these areas should display clockwise rotations in paleomagnetic declination.

2. Geologic setting and sampling

Early Proterozoic supracrustal rocks in the Slave craton are mainly preserved in three basins: the Coronation basin in the northwest, the Kilohigok basin in the northeast, and the Great Slave basin in the south (Fig. 1a; Hoffman, 1973). The Great Slave Supergroup is more than 12-km thick and consists of weakly metamorphosed sedimentary and

Table 1
Summarized paleomagnetic poles of the Coronation APWP.

Basin	Group	Formation	Abbreviation	Age (Ma)	Age reference	Plat (°N)	Plong (°E)	A_{95} (°)	N	Paleomagnetic reference	Local rotation*
Kilohigok		Mara River sills	MRS	1870 ± 1	Davis et al. (2004)	−27	268	0	1	Evans and Hoye (1981)	Unlikely
Kilohigok	Wolverine	Peacock Hills	PH	1882 ± 4	Correlation by Mitchell et al. (2010)	−15	270	11	15	Evans and Hoye (1981)	Unlikely
Kilohigok	Bear Creek	Mara	MA	1885 ± 5	Correlation by Mitchell et al. (2010)	−7	253	7	28	Evans and Hoye (1981)	Unlikely
Kilohigok	Bear Creek	Rifle	RF	1963 ± 6	Bowring and Grotzinger, (1992)	14	341	9	22	Evans and Hoye (1981)	Possible
Coronation		Peninsular sill	PS	1871 ± 1	M.A. Hamilton in Buchan et al. (2010)	−22	263	7	7	Irving and McGlynn (1979)	Unlikely
Coronation		Takiyuak	TK	ca. 1885–1870	Correlation by Mitchell et al. (2010)	−13	249	8	17	Irving and McGlynn (1979)	Unlikely
Great Slave	Christie Bay	Pearson (A)	PE	ca. 1870	Correlation by Mitchell et al. (2010)	−19	283	9	12	McGlynn and Irving (1978)	Unlikely
Great Slave	Christie Bay	Tochatwi	TO	ca. 1885–1870	correlation by Mitchell et al. (2010)	−18	216	12	8	Evans and Bingham (1976)	Likely
Great Slave	Christie Bay	Stark	ST	ca. 1885–1870	Correlation by Mitchell et al. (2010)	−15	212	7	39	Bingham and Evans (1976)	Likely
Great Slave	Pethei	Douglas Peninsula	DP	ca. 1885–1870	Correlation by Mitchell et al. (2010)	−17	258	16	6	Irving and McGlynn (1979)	Unlikely
Great Slave	Kahochella	(K)	KA	1882 ± 4	Correlation by Mitchell et al. (2010)	−7	298	9	18	Reid et al. (1981)	Unlikely
Great Slave	Kahochella	Seton (C)	SE	1885 ± 5	Correlation by Mitchell et al. (2010)	2	267	6	19	Irving and McGlynn (1979)	Unlikely
Great Slave	Sosan	Akaitcho River	AR	1885 ± 5	Correlation by Mitchell et al. (2010)	−4	268	7	35	Evans et al. (1980)	Unlikely
		Ghost dykes	Ghost	1887–1884	Buchan et al. (2016)	2	254	6	23	Buchan et al. (2016)	Unlikely
		Lac de Gras dykes	LdG	2029–2023	Buchan et al. (2009)	12	268	7	10	Buchan et al. (2009)	Unlikely

Notes: Plat = pole latitude, Plon = pole longitude, A_{95} = radius of 95% confidence cone of the pole, N = number of sites. Paleomagnetic poles are listed using values from original papers.
* Mitchell et al. (2010) present a model of 12° rotations based on trans-cratonic structural analyses (not applied here).

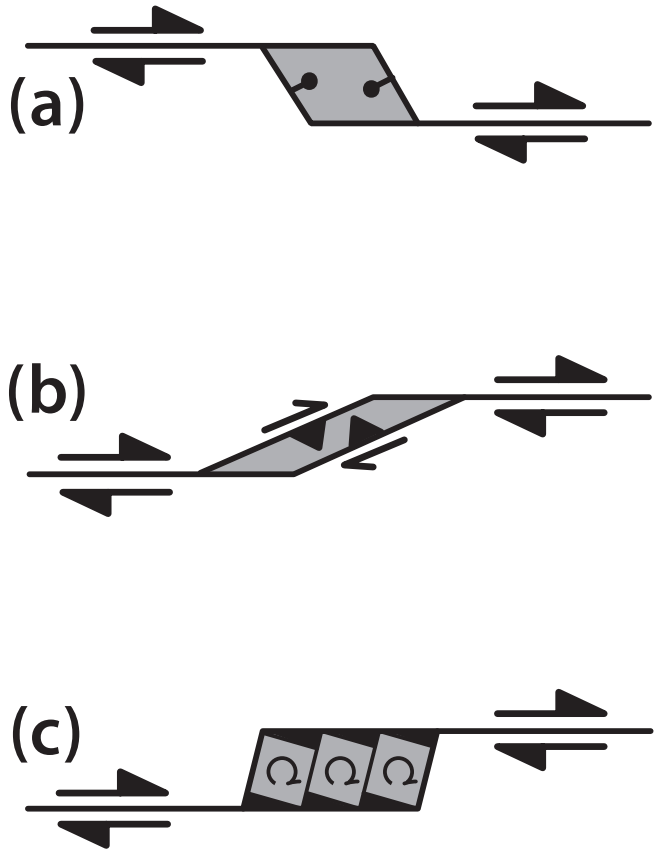

Fig. 3. Styles of structural linkage in segmented dextral strike-slip faults. (a) Right-stepping right-slip faults linked by a pull-apart basin (shaded) or rhombochasm (Carey, 1958; Segall and Pollard, 1980). Ornaments identify the hanging-walls of normal faults. (b) Left-stepping right-slip faults linked by a positive flower structure (shaded; Wilcox et al., 1973). Barbs identify the hanging-walls of oblique reverse faults. (c) Left-stepping right-slip faults linked by a zone of rotated crustal blocks (Kim et al., 2004). Both the blocks (shaded) and their bounding antithetic left-slip faults have rotated clockwise. Block rotation may be augmented by simple-shear rotation of strain axes within the transfer zone as a whole. In addition, individual block rotations will not be quantitatively self-limiting if the blocks become rounded through wear, potentially accounting for rotations > 15°.

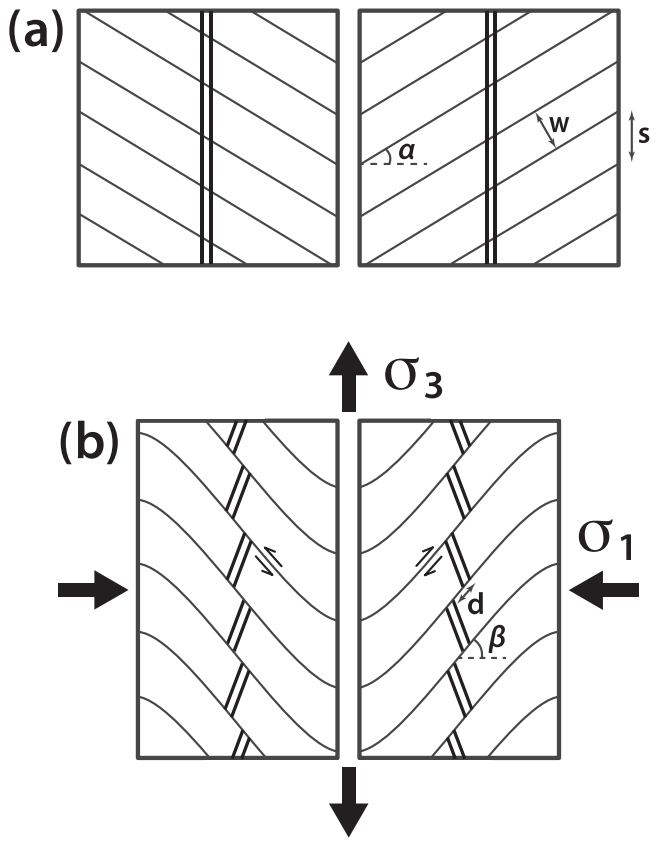

$$s = \frac{w}{\cos\alpha}, \quad (1) \qquad \frac{d}{s} = \frac{\sin(\beta-\alpha)}{\cos\beta}, \quad (2) \qquad \frac{d}{w} = \frac{\sin(\beta-\alpha)}{\cos\alpha\cdot\cos\beta} \quad (3)$$

Fig. 4. Kinematics of conjugate transcurrent faulting (modified after Freund, 1970, 1974). Sinistral (left) and dextral (right) fault domains. (a) Initial condition showing faults (solid lines) with failure angles (α) ~30° relative to the direction of maximum compressive stress (σ_1). Spacing between faults (s) defines fault-block width (w). Passive marker indicated by double line. (b) Condition after 15% shortening. Strain is accommodated by strike-slip displacement (d), proportional to the width and degree of rotation (β-α) of the fault-blocks toward the stretching direction (σ_3) (Eqs. 2 and 3). Note clockwise and counterclockwise rotations of the passive marker (double lines) in sinistral and dextral fault domains, respectively. Fault-block curvature is just one possible means of accommodating loss of displacement toward the fault tips. Splay faulting (not shown) is another.

volcanic rocks. It represents the depositional history of the Great Slave basin at 2.1–1.8 Ga, and is subdivided into five stratigraphic units; from lowermost to uppermost these are the Union Island, Sosan, Kahochella, Pethei and Christie Bay Groups (Stockwell, 1936; Hoffman, 1968). The regional structure of the Great Slave basin is dominated by a doubly-plunging, NNE-trending synclinorium centered on Christie Bay. The synclinorium contains a system of NW-directed, thin- and thick-skinned thrust sheets (nappes) of large displacement. The southern limb of the synclinorium exposes the entire thrust stack, while only the Christie Bay Group is allochthonous on the northern limb due to a frontal thrust ramp. Thrusting predated emplacement of the Compton Intrusive Suite (Hoffman et al., 1977; Hoffman, 1988b), a chain of laccoliths of intermediate composition extending nearly the entire length of the basin (Fig. 1b). The laccoliths are folded within the regional synclinorium, but thrusting and folding were both likely close in age to that of laccolith emplacement, which is best estimated as 1868.46 ± 0.76 Ma based on a preliminary restudy of sample VS 79–10 (Bowring et al., 1984) by S.A. Bowring (pers. comm., 2013). The southern limb of the synclinorium, including the thrust system and the Compton laccoliths, are cut by a parallel system of brittle right-slip vertical faults, the McDonald Fault system (Fig. 1). The fault system accommodates an estimated 65–80 km of right-lateral slip (Thomas et al., 1976; Hoffman et al., 1977; Hoffman, 1981) and has a sinistral conjugate counterpart in the NW-trending Bathurst Fault system (Gibb, 1978; Fig. 1). On a more local scale, the McDonald Fault system is segmented, and the two most prominent segments, the Laloche and McDonald Faults, have a left-stepping relationship (Fig. 1b). Many right-slip (i.e., dextral strike-slip) fault systems have right-stepping segments that are linked by transtensional ("pull-apart") basins (Fig. 3a), aptly named "rhombochasms" by Carey (1958). The left-stepping Laloche-McDonald fault segments are linked by transfer faults that have oblique reverse-slip (Fig. 3b). Upthrusted basement blocks (e.g., Simpson Islands-Hornby Channel area, Fig. 1b) are flanked by steeply dipping footwall monoclines of Paleoproterozoic sedimentary strata, creating a "positive flower structure" as observed in Cenozoic transpression zones (Lowell, 1972; Wilcox et al., 1973). The difference in structural behavior, one producing a sediment sink and the other a sediment source, relates to the stress field around the fault tip. The left side of a dextral fault tip is in compression, while the right side of the fault tip is in tension (Segall and Pollard, 1980).

Some left-stepping dextral fault systems (Fig. 3c) have overlapping fault segments linked by zones where small blocks have been rotated

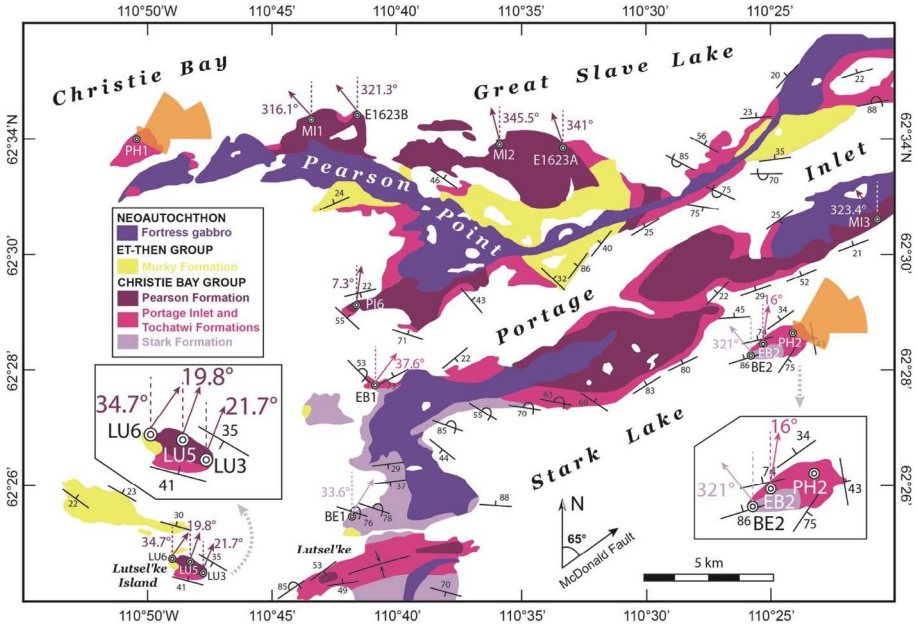

Fig. 5. Geologic map of part of the East Arm of Great Slave Lake (modified after Hoffman, 1988b). Inset table is the stratigraphic column. Bedding strikes are shown with numbers indicating the degree of tilting (dip > 20° only). Pearson Point strata are shallowly dipping. Arrows are paleomagnetic remanence declinations after tilt-correction from: the Pearson Formation (sites LU3, LU5, LU6, PI6, E1623A, and E1623B are from this study and sections MI1, MI2, MI3 are from McGlynn and Irving, 1978), the Stark Formation (section BE1 and site BE2 of Bingham and Evans, 1976), and the Tochatwi Formation (section EB1 and site EB2 from Evans and Bingham, 1976). Section declinations represent averages of several sites. Rose diagrams are paleocurrent azimuths of the Tochatwi Formation (sections PH1 and PH2 from Hoffman, 1969). Black arrow shows the dominant trending direction of the McDonald Fault system.

clockwise, along with their bounding antithetic left-slip faults (Kim et al., 2004). The strain field between the fault segments is similar to that of "flower structures", but limited exclusively to the horizontal plane. One of the best-documented cases of clockwise rotation in such a setting is the Transverse Ranges left-step on the San Andreas Fault in southern California (Hornafius et al., 1986).

Oblique "*en echelon* folds" (Wilcox et al., 1973) of northeasterly trend and gentle plunge are widely observed along the McDonald Fault system. They are most easily observed in the Et-Then Group, an assemblage of syn-kinematic alluvial fanglomerate and sandstone (Stockwell, 1932; Hoffman, 1969; Ritts and Grotzinger, 1994), which unconformably overlies the Great Slave Supergroup and postdates thrusting, laccolith emplacement and folding of the regional syncline. These *en echelon* folds manifest a resolved component of dextral transpression in the fault system, consistent with its wholescale rotation (see text below). The plunging folds create the structural relief that exposes the architecture of the thrust stack, and controls its expression on a geological map (Hoffman, 1988b).

The conjugate McDonald and Bathurst Fault systems are kinematically homologous with a pervasive system of smaller-scale conjugate transcurrent faults in the Wopmay orogen (Cook, 2011; Hildebrand, 2011). The conjugate fault system in the Wopmay orogen postdates the youngest plutons of the Great Bear magmatic arc (Fig. 1a), which are dated around 1.84 Ga (Bowring, 1985; Hildebrand et al., 2010), and predates the 1.74 Ga Cleaver dykes (Hildebrand, 1985; Irving et al., 2004). The conjugate system accommodated east-west shortening by north-south lengthening (Fig. 4), implying the existence of a free face (active subduction zone) to the north or south. The strain is attributed to terminal collision in the Wopmay orogen (Hoffman, 1980; Hildebrand, 1987; Cook, 2011). Structural homology and permissive chronology underlie the conjecture (Hoffman, 1980, 1988b) that conjugate transcurrent faulting in the Wopmay orogen is cogenetic with the Bathurst-McDonald Fault systems far to the east. This conjecture remains untested because the age of the Bathurst and McDonald Fault displacements are too weakly constrained.

Conjugate transcurrent fault systems (Fig. 4) have been analyzed in analog models and Cenozoic examples (Cloos, 1955; Freund, 1970, 1974). Regional bulk strain is accommodated on brittle faults by fault-block rotations (Fig. 4b). Conjugate faults have original failure angles ~30° with respect to the maximum shortening direction (σ_1), which is close to east-west in the Wopmay and Bathurst-McDonald examples. Those faults rotated toward the stretching direction (north-south, σ_3) as strain accumulated: dextral faults rotated counterclockwise and sinistral faults clockwise (Fig. 4b). In the foreland of the Wopmay orogen, Calderian folds and thrusts that predate strike-slip faulting (equivalent to the double lines in Fig. 4) trend north-south in areas where strike-slip faults are absent. These same structures were rotated clockwise or counterclockwise equivalently in domains where strike-slip faulting occurs (Hoffman, 1994). This demonstrates a regional pure shear (irrotational strain) regime (Fig. 4b), despite a strong prevalence in Wopmay orogen of dextral over sinistral fault domains.

The angle between the Bathurst and Macdonald Fault trends is close to 84°, implying that this angle widened by ~24° assuming initial failure angles of ~30° for each fault. This implies that the fault systems have each rotated by an average of 12°, the Bathurst in a clockwise direction and the McDonald counterclockwise (Mitchell et al., 2010). Such rotations apply to the fault systems as a whole. They do not necessarily describe rotations of small blocks within the fault zones (Fig. 3c; Kim et al., 2004), except in the case of the Wopmay orogen where the conjugate fault kinematics appear to be self-similar on all scales (Tirrul, 1992; Hoffman, 1994). As the Bathurst and McDonald Faults rotated toward the σ_3 (north-south) direction, the normal-stress component on the fault planes increased (Fig. 4b). This resulted in the development of transpressional structures such as *en echelon* folds (Wilcox et al., 1973). It also limited the amount of rotation that could be achieved, because block rotation renders the fault planes progressively less favorable for strike-slip displacement (Freund, 1970, 1974).

The Pearson Formation is the uppermost member of the Christie Bay Group (Fig. 5), and experienced the early phases of deformation as described above. It is characterized by basalt flows and occurs stratigraphically between the conformably underlying Portage Inlet Formation (Christie Bay Group) and the unconformably overlying Et-Then Group. Columnar joints and (rarely) pillow structures have been observed in the field (Stockwell, 1932; Barnes, 1951). The Pearson Formation is provisionally correlated with the 1871 ± 1 Ma Peninsular sill in the Coronation basin (M.A. Hamilton in Buchan et al., 2010) and the 1870 ± 1 Ma Mara River sills in the Kilohigok basin (Davis et al., 2004). Such a correlation would imply that the Pearson lavas are a few million years older than the Compton laccoliths, a reasonable supposition but untestable as the two are nowhere in contact. The Pearson Formation is limited in preservation to the central part of the Christie Bay syncline (Fig. 5), where it reaches a maximum thickness of 168 m

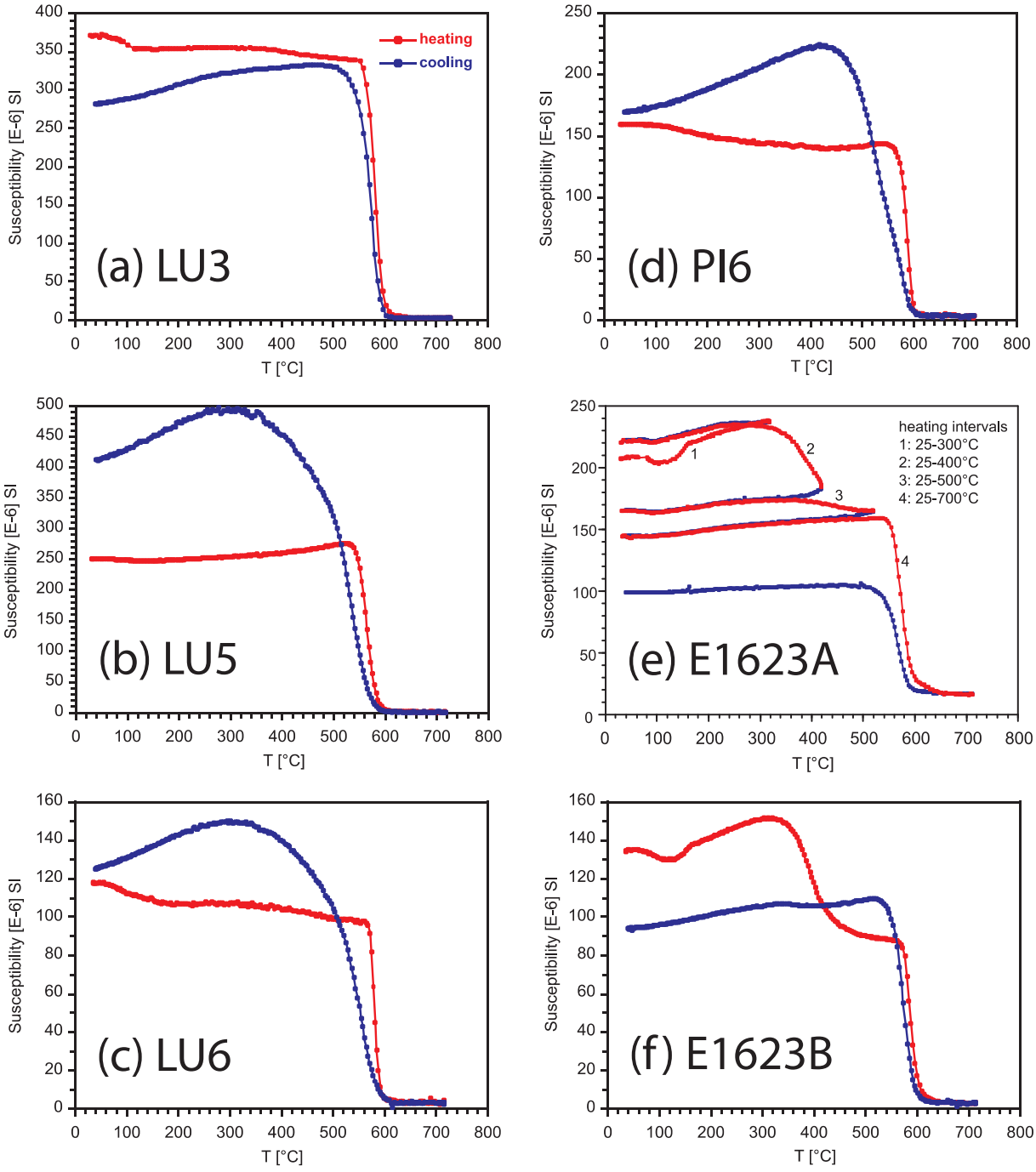

Fig. 6. Thermomagnetic susceptibility experiment of the Pearson Formation. Red and blue lines represent heating and cooling curves, respectively. (For interpretation of the references to colour in this figure legend, the reader is referred to the web version of this article.)

(Barnes, 1953). The lavas are amygdaloidal or vesicular; plagioclase (albite) is saussuritized and pyroxene is replaced by actinolite or chlorite (McGlynn and Irving, 1978). Opaque minerals in the basalts are dominated by magnetite, with minor amounts of maghemite and pyrite. The maximum burial temperature of the Pearson Formation is about 250–350 °C, which is inferred from prehnite-pumpellyite facies metamorphism (McGlynn and Irving, 1978).

Previous paleomagnetic study of the Pearson Formation includes samples collected from Pearson Point and northern shoreline of the Stark Lake (sections MI1, MI2, MI3 in Fig. 5), where the Pearson Formation is gently folded (dip $< 20^{\circ}$) about NE-trending axes, consistent with the large-scale structure of the Great Slave basin (McGlynn and Irving, 1978). However, no information regarding the stratigraphic positions of those previous samples is available. For comparison with the results of McGlynn and Irving (1978), we sampled two sites at northern Pearson Point (E1623A and E1623B; Fig. 5) from the basal Pearson Formation in direct contact with the underlying Portage Inlet Formation.

To test the vertical-axis rotation hypothesis for published paleomagnetic data from the Christie Bay Group, we sampled the basal Pearson Formation in areas where the structures deviate from the typical NE trend. One site (PI6) is at the mouth of Portage Inlet and three sites (LU3, LU5, LU6) are on Lutsel'ke Island (Fig. 5). Lutsel'ke Island samples were collected from opposing limbs of a syncline for paleomagnetic fold test. Paleomagnetic samples were oriented in the field using a Brunton compass and were further checked with a sun compass

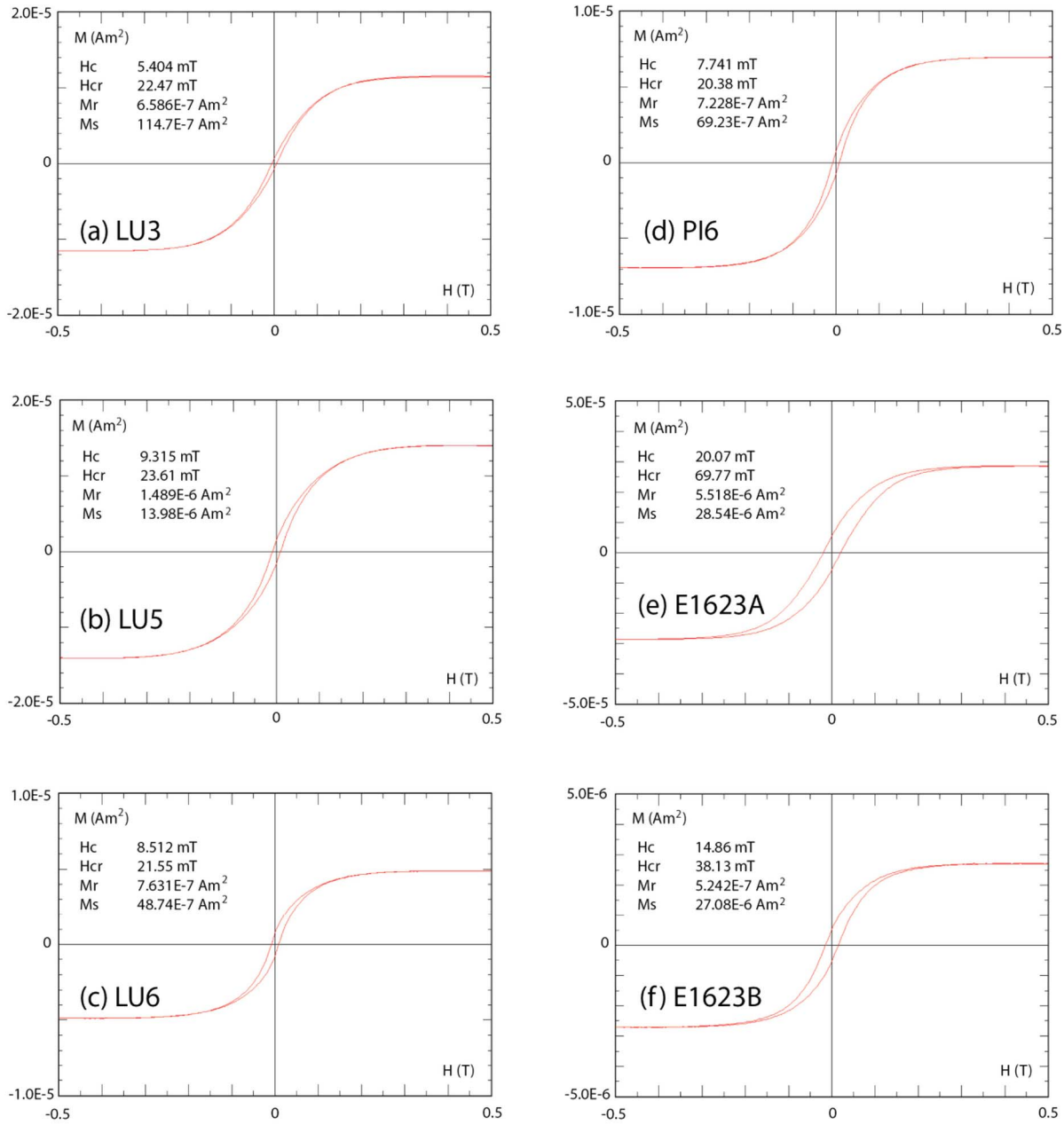

Fig. 7. Hysteresis loops of the Pearson Formation after paramagnetic slope correction.

whenever possible. Measured magnetic deviations (~17°E) were found to be consistent with those calculated from the International Geomagnetic Reference Field (IGRF) model. Oriented samples were trimmed to a uniform size (2.5 cm in diameter, 1.2 cm in length) for laboratory measurements. Rock chips were prepared for rock magnetic analyses.

3. Magnetic measurements

Rock magnetism was studied on representative Pearson samples from each site. In order to identify magnetic mineralogy by Curie/Néel temperature, the bulk magnetic susceptibility was measured during both heating and cooling between 25 °C and 700 °C in an argon gas environment with an AGICO Kappabridge KLY-4S susceptibility meter and a CS3 high temperature furnace apparatus. Additionally, magnetic parameters, including coercivity (Hc), coercivity of remanence (Hcr), saturation magnetization (Ms) and saturation remanence (Mr), were determined by hysteresis loop measurements, which were acquired from −0.5 T to 0.5 T at steps of 4 mT using a Princeton Measurements Corporation MicroMag 2900 alternating gradient magnetometer (AGM) at the Yale University Archaeomagnetism Laboratory. Paramagnetic slope correction was applied for all hysteresis loops.

Demagnetization of the Pearson samples was conducted in a magnetostatically-shielded room (ambient field intensity < 300 nT) at the Yale University Paleomagnetism Laboratory. After the measurement of natural remanent magnetization (NRM), samples were submerged in liquid nitrogen (~77 K) in a shielded cylinder for ≥30 min in order to remove the remanence carried by larger magnetic grains, following Muxworthy and McClelland (2000). Then samples were thermally demagnetized, progressively from 100 °C to 580 °C in about 20 steps in a nitrogen gas environment using an ASC Scientific TD-48 thermal demagnetizer. Remanences were measured by a 2G Enterprises DC-SQUID magnetometer with an automated sampling-changing vacuum system (Kirschvink et al., 2008). Paleomagnetic data were plotted using vector-endpoint diagrams (Zijderveld, 1967) in PaleoMag X (Jones, 2002).

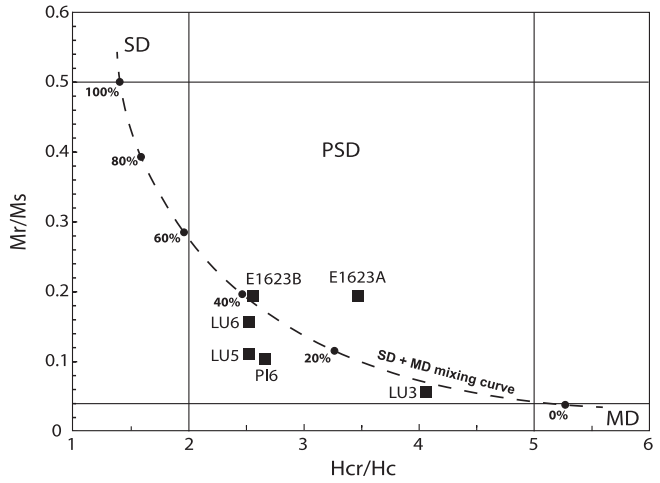

Fig. 8. Day plot (Day et al., 1977) of the Pearson Formation. Dashed line represents the theoretical mixing curve for MD grains at different percentages (black dots) with SD magnetite (Dunlop, 2002). The SD, PSD, and MD regions are from Dunlop (2002).

Principal component analysis (PCA) was used to determine the remanence components of each sample (Kirschvink, 1980). Fisher statistics were used to calculate mean paleomagnetic directions in Stereonet (Cardozo and Allmendinger, 2013). Paleomagnetic poles were calculated following Butler (1992) and were plotted in GPlates (Boyden et al., 2011).

4. Results

4.1. Magnetic mineralogy

Thermomagnetic susceptibility curves of representative Pearson samples from all six sites are characterized by abrupt loss of bulk magnetic susceptibility at 580–590 °C during heating (Fig. 6), supporting the presence of magnetite (Curie temperature 585 °C). Most thermomagnetic susceptibility curves are not reversible. The difference between heating and cooling curves is possibly due to magnetic phase transitions that occurred during thermal treatments, although the argon gas environment should have subdued chemical reactions. Different from other sites, Pearson Point samples (sites E1623A and E1623B) show three distinct susceptibility reductions at ~100 °C, ~350 °C and ~580 °C, which are close to the Curie/Néel temperatures of goethite, pyrrhotite and magnetite, respectively (Fig. 6e and f). The cooling curves of Pearson Point samples are much lower than the heating curves, indicating significant loss of ferromagnetic composition. In order to determine at what temperature the magnetic phase transitions took place, we heated Pearson Point samples in multiple temperature intervals, specifically at 25–300 °C, 25–400 °C, 25–500 °C and 25–700 °C. The major decrease of magnetic susceptibility occurred at 300–400 °C and 500–600 °C, with a moderate loss at 400–500 °C. However, the complicated pattern of magnetic mineralogical change was not observed in thermal demagnetization of any Pearson Point samples (Fig. 9e and f). Thus, it is safe to regard magnetite as the dominant carrier of remanence for all Pearson samples (see discussion below).

Hysteresis loops of the Pearson samples show that the magnetization is saturated between 0.2 T and 0.3 T, and the coercivity of remanence is less than 70 mT, with a typical value of 30 mT (Fig. 7). The Mr/Ms. and Hcr/Hc ratios were plotted to study magnetic grain size distribution (Day et al., 1977). All Pearson samples fall into pseudo-single domain (PSD) range in the Day plot (Fig. 8). The morphology of the hysteresis loop also agrees with the behavior of PSD grains (Tauxe, 1998). Based on the theoretical experiments of Dunlop (2002), the PSD signature results from the mixing of single domain (SD) and multidomain (MD) grains. Inferred from the Day plot, the Pearson samples contain about 20–40% of SD grains, except for site LU3, which has less (~10%) SD grain contribution (Fig. 8).

4.2. Paleomagnetic results

Nearly all Pearson samples carry single magnetization components decaying towards the origin on vector-endpoint diagrams (Fig. 9), which are defined as their characteristic remanent magnetizations (ChRMs). The unblocking temperatures of the ChRMs are at 540–580 °C, with square-shouldered pattern on thermal demagnetization curves (Fig. 9). Viscous overprints carried by multidomain grains were adequately removed by either liquid nitrogen bath or low temperature heating.

4.2.1. Lutsel'ke Island

Three sites (LU3, LU5, LU6 in Fig. 5) collected from the syncline on Lutsel'ke Island provide an opportunity for paleomagnetic fold test to determine the age of remanence acquisition (Fig. 10a). Before any tilt correction, site means are very distinct. ChRMs from sites LU3 and LU5 are directed upwards to the northeast and the ChRM from site LU6 is directed downwards to the south (Fig. 10b). A paleomagnetic fold test (Enkin, 2003) was performed, and the largest precision parameter (k) is achieved at 110–115% unfolding, indicating a better clustering after tilt correction (Fig. 10c and d). The in-situ and tilt-corrected site means and their corresponding virtual geomagnetic poles (VGPs) are shown in Figs. 10 and 12, respectively.

4.2.2. Mouth of Portage Inlet

Site PI6 (Fig. 5) was collected at the entrance to Portage Inlet, which gives an in-situ site mean of $Dec_G = 11.1°$, $Inc_G = -26.7°$ ($\alpha_{95} = 10.3°$, k = 35.7; Fig. 11a). The tilt-corrected site mean is $Dec_S = 7.3°$, $Inc_S = -25.1°$ ($\alpha_{95} = 10.3°$, k = 35.7; Fig. 11b), and the corresponding VGP is located at 14.1°S, 242.0°E ($A_{95} = 8.1°$; Fig. 12).

4.2.3. Pearson point

Previous paleomagnetic study of the Pearson Formation was conducted at Pearson Point (sections MI1 and MI2 in Fig. 5), as well as areas on northern shoreline of Stark Lake (section MI3 in Fig. 5; McGlynn and Irving, 1978), which provides a tilt-corrected mean direction of $Dec_S = 329°$, $Inc_S = -8°$ ($\alpha_{95} = 10°$; Fig. 11b) and a corresponding paleomagnetic pole at 19°S, 283°E ($A_{95} = 9°$; Fig. 12). We collected another two sites (E1623A and E1623B) from the basal Pearson Formation at Pearson Point (Fig. 5), broadly the same area as McGlynn and Irving (1978). The site means of these two sites, after tilt correction, fall close to the 95% confidence cone of the previous mean direction (Fig. 11). The slight difference could be explained by paleosecular variation or the uncertainties generated in sampling and/or measurements.

All paleomagnetic results of the Pearson Formation are summarized in Table 2. It is noteworthy that the tilt-corrected site means of six sites show prominent differences in paleomagnetic declination, but not significant differences in paleomagnetic inclination. In general, the declinations of Lutsel'ke Island and Portage Inlet samples are directed to the northeast, while declinations of Pearson Point samples are directed to the northwest.

5. Discussion

5.1. Remanence carrier and age of remanence acquisition

The dominant magnetic phase in Portage Inlet (PI6) and Lutsel'ke Island (LU3, LU5 and LU6) samples is magnetite, which is supported by the Curie temperature (580–590 °C) determined in the thermomagnetic susceptibility experiments (Fig. 6a–d). In contrast, Pearson Point (E1623A and E1623B) samples may contain multiple magnetic phases

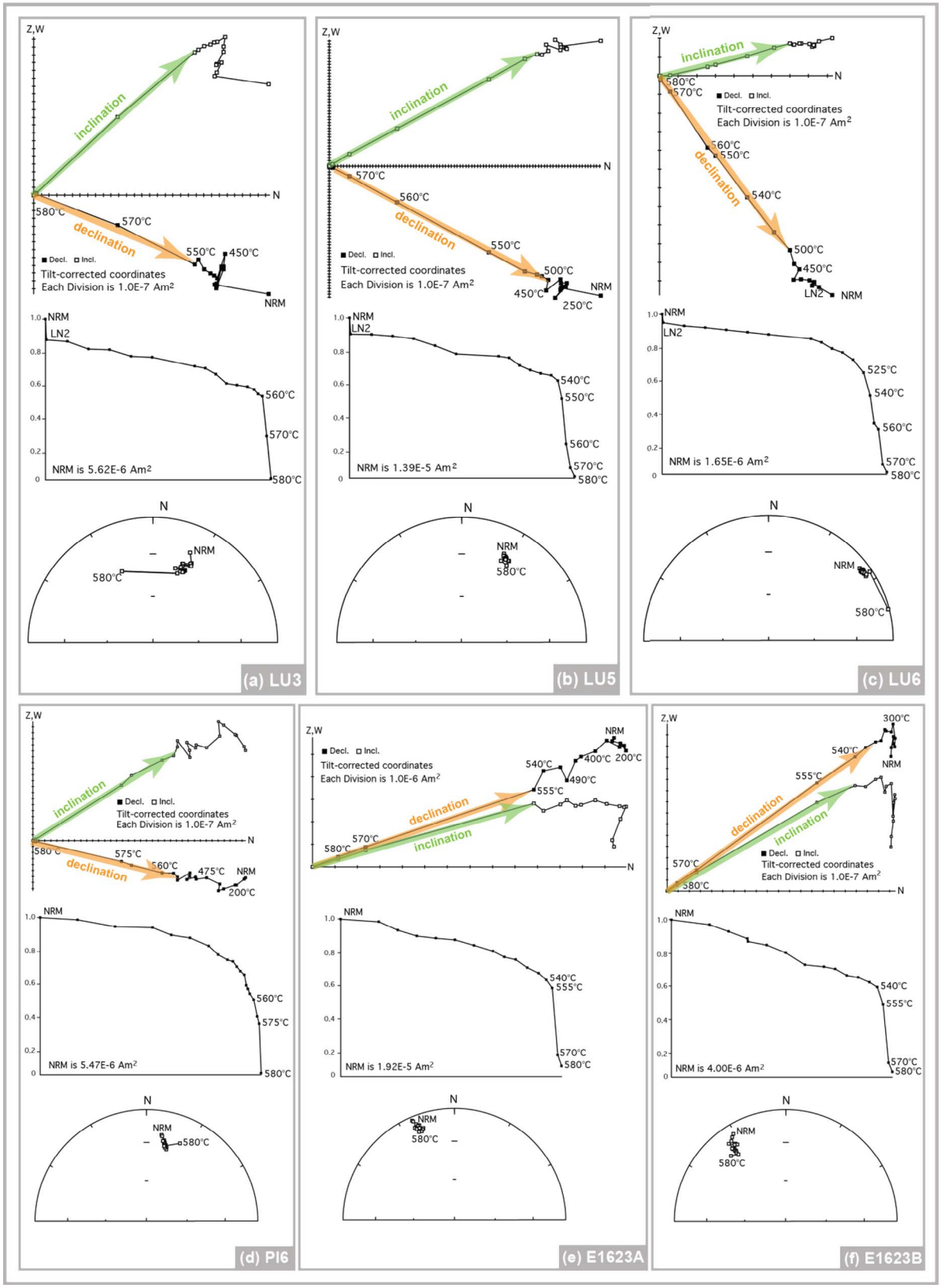

Fig. 9. Representative thermal demagnetization of the Pearson Formation. Typical vector-endpoint diagrams (Zijderveld, 1967), remanence intensity (J/J_0) plots, and equal-area stereonet plots are shown for each site. Vectors determined with least-squares analysis of magnetization components (Kirschvink, 1980) are plotted with orange and green arrows representing paleomagnetic declinations and inclinations, respectively. (For interpretation of the references to colour in this figure legend, the reader is referred to the web version of this article.)

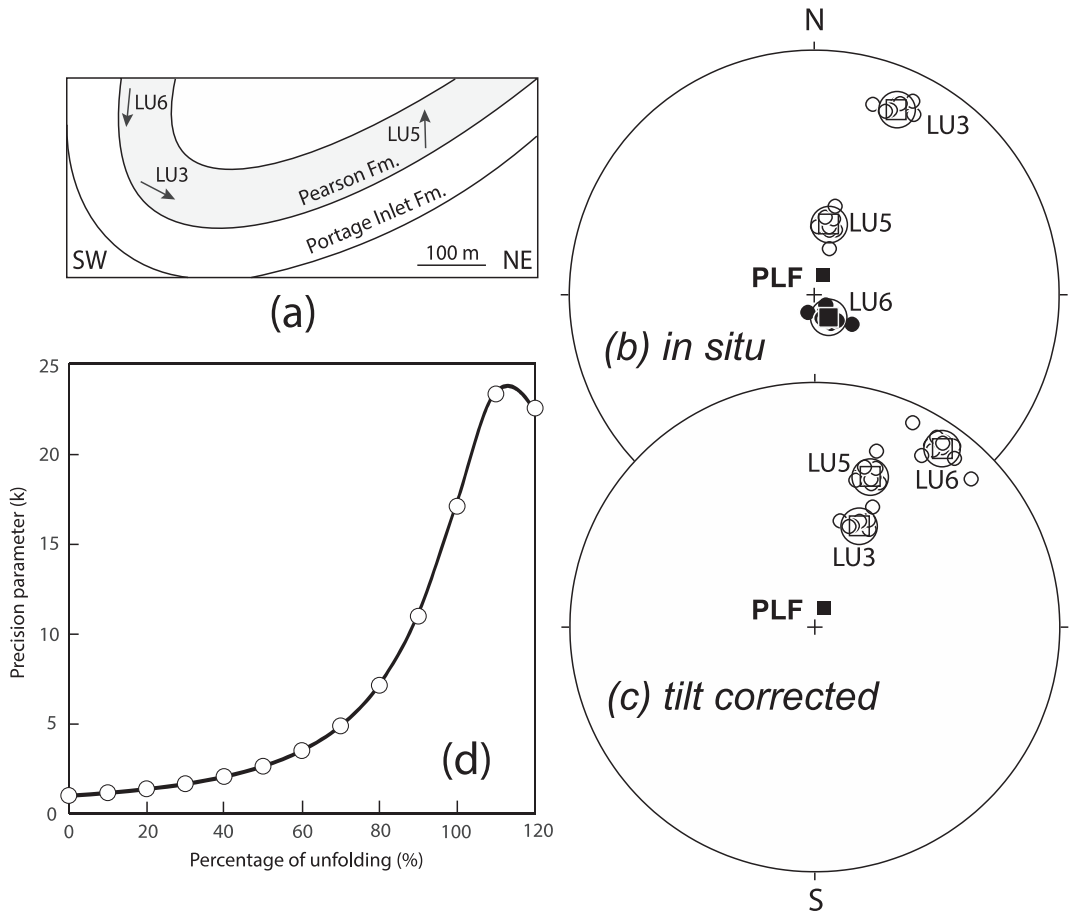

Fig. 10. (a) Schematic illustration of the paleomagnetic fold test conducted on Lutsel'ke Island with site location and stratigraphic relations indicated. Black arrows show site-mean inclinations before tilt correction. Equal-area stereonets of site means (b) before tilt correction and (c) after 100% tilt correction. Mean directions are shown with 95% confidence cones. Open (filled) circles are in upper (lower) hemisphere. Present-local field (PLF) direction is represented by the square. (d) Stepwise unfolding (Enkin, 2003) shows that the maximum precision parameter (k) is achieved at 110–115% unfolding.

since several different Curie/Néel temperatures have been identified on thermomagnetic susceptibility curves (Fig. 6e and f). Prominent decreases of bulk magnetic susceptibility at ~100 °C, ~350 °C and ~580 °C on heating curves indicate the presence of goethite, pyrrhotite and magnetite, respectively. Previous mineralogical study of the Pearson samples shows the presence of maghemite and pyrite (McGlynn and Irving, 1978). Except for paramagnetic pyrite, other magnetic minerals are ferromagnetic and could be potential remanence carriers.

Results from thermal demagnetization show that all Pearson samples yield a single magnetization component that is defined as the ChRM. The unblocking temperature of the ChRMs of the Pearson samples is at 540–580 °C, close to the Curie temperature of magnetite (Fig. 9). No other unblocking temperature was observed corresponding to the Curie/Néel temperatures determined in thermomagnetic susceptibility experiments. Hence, it is important to point out that none of goethite, pyrrhotite or maghemite, if they exist, produces any significant contribution to the ChRMs of the Pearson samples.

The difference between the Curie temperature and the unblocking temperature of the magnetite in the Pearson samples likely originates from the grain size, instead of high titanium content. Larger grains, especially MD grains, have lower unblocking temperatures and yield less stability compared to SD grains (Butler, 1992). The presence of MD/PSD grains is indicated by the hysteresis loop patterns and the Day plot (Figs. 7 and 8), but the remanence contributed by MD grains should be adequately removed by liquid nitrogen bath or thermal demagnetization at low temperatures. Therefore, the ChRMs of Pearson samples are carried by SD or small PSD magnetite grains, of which the remanences have significant temporal stability.

The square-shouldered pattern exhibited at the unblocking temperature is observed in thermal demagnetization curves (Fig. 9), which suggests a thermoremanent magnetization. Additionally, there is no evidence for chemical remagnetization. Authigenic magnetite produced by chemical alterations normally shows a gradual decay of remanence intensity during thermal demagnetization. Influences of lightning (isothermal remanent magnetization) are also unlikely since the NRM intensities of Pearson samples are of typical values (10^{-5}–10^{-6} Am^2) for basalts. Besides, the overprint yielded by lightning would also show a gradual decrease in remanence intensity as temperature increases, so the square-shouldered pattern at high temperatures (nearly 580 °C) should not be expected. The in-situ ChRMs of the Pearson samples are notably distinct from the present-local field (PLF) direction (Figs. 10 and 11). The most likely tectonomagmatic events that may have had the potential to remagnetize the strata in the Great Slave basin is the Coronation (or more broadly, Trans-Hudson) orogenesis at ca. 1750 Ma and intrusion of the Mackenzie large igneous province at ca. 1270 Ma (Irving et al., 1972; Evans and Bingham, 1976; Evans et al., 1980; Reid et al., 1981). Neither of those well-defined directions is observed in the Pearson samples. Most importantly, the age of remanence acquisition is constrained by the fold test of Lutsel'ke Island samples. The site means of Lutsel'ke Island samples achieve best grouping at 110–115% unfolding, slightly over 100% (Fig. 10), which is perhaps attributable to paleosecular variation, unrecognized primary dips of the volcanic strata, uncertainties in bedding measurements (bedding of site LU6 was measured on glacial-polished surfaces of pillow basalts, which might be less accurate), or other possible minor sources of systematic error. Thus, the fold test is regarded as positive, confirming a pre-folding origin of

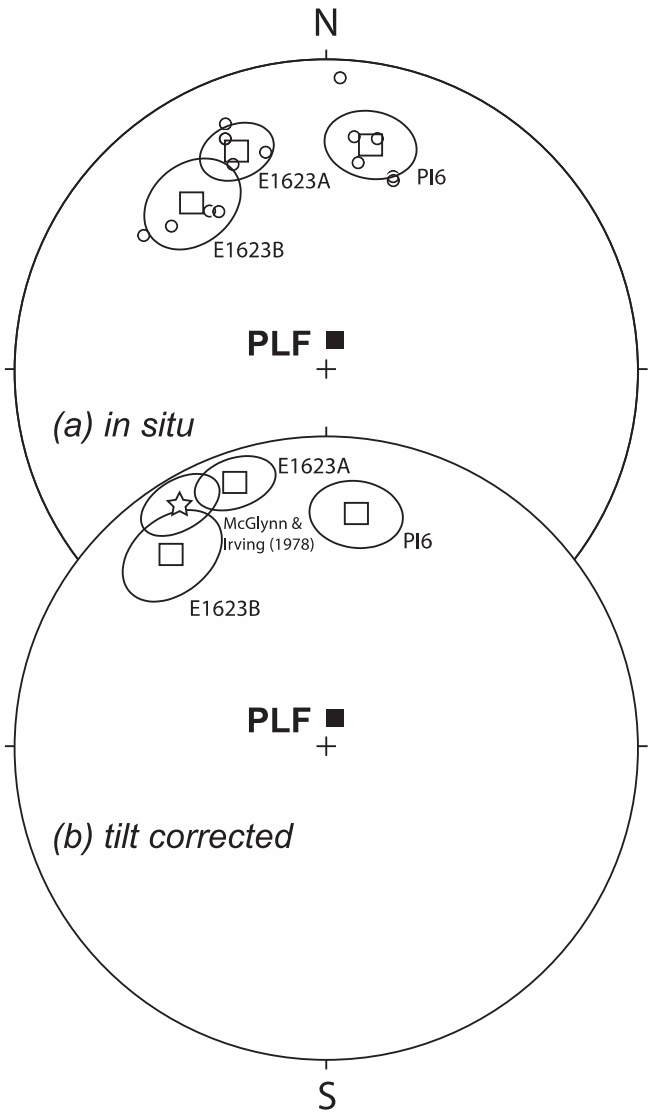

Fig. 11. Equal-area stereonets of site means from two sites at Pearson Point and one site at the mouth of Portage Inlet (a) before tilt correction and (b) after tilt correction. Mean directions are shown with 95% confidence cones. Open circles are in upper hemisphere. Present-local field (PLF) direction is represented by the yellow square. Star represents the previous result of McGlynn and Irving (1978).

the remanence. Since folding does not penetrate the overlying Et-Then Group (Barnes, 1951), with an age of ca. 1780 Ma estimated by stratigraphic correlation (Mitchell et al., 2010), the ChRM of the Pearson Formation was likely acquired during the initial cooling of the basalts and represents a primary thermoremanent magnetization.

5.2. Variations in the Pearson Formation magnetization directions

Tilt-corrected paleomagnetic results from the Pearson samples collected here yield several discordant directions, and correspondingly, several isolated VGPs (Fig. 12). We note that the discordance of the paleomagnetic directions is largely due to the differences in declination, with relatively small variations in inclination. To explain the discordant paleomagnetic data, we first test the vertical-axis rotation hypothesis, and then discuss the plausibility of other possible explanations.

5.2.1. Vertical-axis rotation

Because the sense of the McDonald Fault is right-lateral (Fig. 1), localized vertical-axis rotations in the proximity to the fault are expected to be clockwise (Kim et al., 2004). In the Great Slave basin, the predominant structural trends are NNE to NE, parallel to the regional syncline and to the McDonald Fault system with varying degrees of obliquity (e.g., transfer faults, flower structures and *en echelon* folds). Northeastward-dipping strata are common in the Et-then Group (e.g., between McDonald Lake and Murky Channel, Fig. 1b), but dips are generally modest (< 40°) as they relate to gently northeastward-plunging *en echelon* folds. Locally, however, steeply-dipping panels of the Pearson Formation and even tight upright folds strike northwest, at odds with regional structural trends. Two such areas are Lutsel'ke Island and the mouth of Portage Inlet (Fig. 5). If related to clockwise block rotation, the rotations would have to be large (~60°) to account for the aberrant structural trends.

To evaluate the vertical-axis block rotation hypothesis (Fig. 3c), a paleomagnetic reference direction is needed to calculate the declination difference between areas. We chose the previous remanence direction of McGlynn and Irving (1978) as a reference because of its relative tectonic stability, as well as its agreement with paleomagnetic results of presumably contemporaneous Peninsular sill (Irving and McGlynn, 1979) and Mara River sills (Evans and Hoye, 1981; Fig. 12) obtained from other regions of Slave craton. If interpreted in this manner, declination anomalies of the Pearson paleomagnetic declinations show 38.3° ± 9.8° clockwise rotation of site PI6 at the mouth of Portage Inlet; and 52.7° ± 7.5°, 50.8° ± 7.5° and 65.7° ± 7.4° clockwise rotations of sites LU3, LU5 and LU6 on Lutsel'ke Island, respectively (Fig. 12a; Table 2). We compared the differences of the structural attitudes with the differences of the paleomagnetic declinations. The rotation of paleomagnetic declination as a function of bedding strike is illustrated in Fig. 12b. Within uncertainties, there is a direct one-to-one correlation between paleomagnetic declinations and deviations of local strike from the McDonald Fault. Hence, the Pearson data are consistent with significant, localized vertical-axis rotation of small blocks in the Great Slave basin.

5.2.2. True polar wander

Earth is a quasi-rigid, self-gravitating planet, which spins with respect to its maximum inertial axis (Gold, 1955). True polar wander (TPW) is excited due to changes in Earth's mass distribution. Studies show that TPW occurs at the velocity of < 1°/Myr (< 11 cm/yr) since late Cretaceous (e.g., Steinberger et al., 2017). But it is suggested that if the Earth's maximum and intermediate moments of inertia are nearly equal, inertial interchange can quickly take place due to the relative waxing and waning of two principal inertial axes (Evans, 1998). Inertial interchange true polar wander (IITPW) could produce rapid back-and-forth rotations of the entire solid Earth around the stable minimum inertial axis in order to realign the new maximum moment of inertia with the spin axis (Raub et al., 2007). The rate of any TPW event is controlled by the viscosity of the mantle, as the planet must deform through its rotational bulge (Tsai and Stevenson, 2007; Creveling et al., 2012; Rose and Buffett, 2017). Geodynamic models show that, theoretically, the rate of TPW could be as fast as ~6° per Myr (Spada et al., 1992; Rose and Buffett, 2017). Mitchell et al. (2010) suggest that the Coronation APWP could be a product of multiple IITPW events when the Slave craton was located close to Earth's minimum inertial axis. However, fast, rate-limited IITPW appears not to be fast enough to explain the ~60° difference observed within broadly coeval Pearson VGPs. Even if we assume that IITPW were faster in Paleoproterozoic time due to a hotter and less viscous mantle (Tsai and Stevenson, 2007), at least ~3 Myr would be required to accommodate the ~60° difference. However, the maximum thickness of the Pearson basalt is only 168 m (Barnes, 1953) and the samples were collected at broadly similar stratigraphic levels within ~20 km lateral distance from each other. Thus, it is considered unlikely that the age difference between the Pearson VGPs is on the order of several million years. The Pearson sites collected here therefore do not support IITPW because the implausibly high rates of motion are implied.

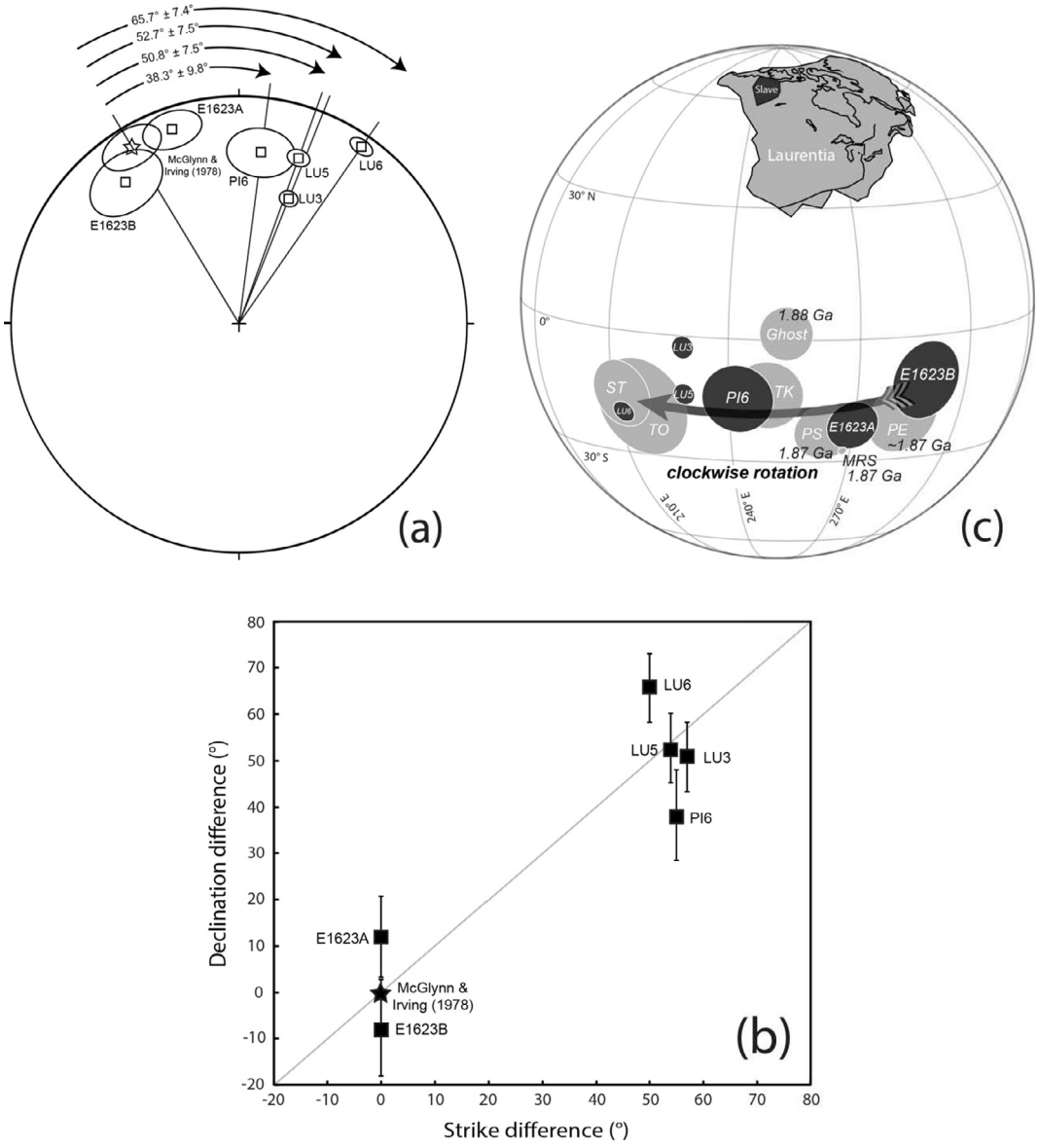

Fig. 12. (a) Difference of the Pearson paleomagnetic declination between sites with respect to the result of McGlynn and Irving (1978) as a reference. Clockwise rotations and 95% confidence limits (R ± ΔR) are calculated following Butler (1992). (b) Paleomagnetic declination deviations are plotted against tectonic strike deviations. The reference declination used to calculate paleomagnetic deviations is that of McGlynn and Irving (1978). The reference strike line used to calculate tectonic deviations is the average trend of the McDonald Fault. Grey line of unit slope is expected if declination deviation is entirely due to vertical-axis rotation. (c) Stereographic projection of Christie Bay Group and correlative paleomagnetic poles (abbreviations as in Fig. 2), the 1885 Ma Ghost dykes pole (Buchan et al., 2016), and our new site-mean VGPs for the Pearson Formation. Arrow indicates the sense of inferred localized rotation of the Pearson Formation VGPs.

5.2.3. Paleosecular variation or non-GAD field

Fast cooling of the Pearson basalts is suggested by pillow lavas and columnar joints observed in the field, implying that each of the Pearson VGPs records a snapshot of the ancient magnetic field. Secular variation of the geodynamo, seemingly stochastic change of both field direction and intensity on short time scales (1–100 kyr; Cox and Doell, 1964), is thus probably not adequately averaged-out at the site (VGP) level. Studies of the recent magnetic field show that paleosecular variation rarely exceeds 30° in direction (Verosub, 1988). Paleosecular variation is thus unlikely to be the cause of the ~60° difference in Pearson declinations. A time-averaged non-GAD field ca. 1.9 Ga is another potential explanation for the Pearson data. In such a model, it can be hypothesized that during magnetic reversals, the dipole field could migrate away from the polar region and could shortly stabilize at a specific location before moving to the opposite polar region (Hoffman, 1991). This kind of non-GAD model has been used to interpret incompatible paleomagnetic directions observed in Laurentia, Baltica and Gondwana in Ediacaran time (Abrajevitch and Van der Voo, 2010; Halls et al., 2015). But it is important to point out that neither the non-GAD field nor the paleosecular variation hypotheses is expected to produce the one-to-one correlation between the declinations and bedding strikes of the Pearson samples.

5.3. Implications for the Coronation APWP

The new results from the Pearson Formation shed light on the Coronation APWP. It is noted that the paleomagnetic poles obtained from the Stark and Tochatwi Formations of the Christie Bay Group lie substantially west of the majority of the Coronation poles (Fig. 2). Furthermore, the paleomagnetic poles obtained from Lutsel'ke Island samples lie close to the Stark and Tochatwi poles (Fig. 12c), raising the question of whether blocks containing Stark and Tochatwi sites have

Table 2
Summarized paleomagnetic results of the Pearson Formation.

Site	n	GPS location		Bedding		In-situ site mean			Tilt-corrected site mean			VGP			Rotation		
		Latitude	Longitude	Strike (°)	Dip (°)	Dec_G (°)	Inc_G (°)	α_{95} (°)	Dec_S (°)	Inc_S (°)	α_{95} (°)	Plat (°N)	Plon (°E)	A_{95} (°)	Structural attitude (°)	Strike difference (°)	Dec difference (R ± ΔR)
LU3	8	62°24′36.10″N	110°48′26.50″W	299	31	23.4	−9.9	2.8	21.7	−40.7	2.8	−2.6	229.3	2.6	119[1]	54	52.7 ± 7.5
LU5	10	62°24′57.60″N	110°48′54.00″W	122	35	10.9	−57.6	3.2	19.8	−23.9	3.2	−13.5	229.3	2.5	122[1]	57	50.8 ± 7.5
LU6	12	62°24′58.70″N	110°49′39.60″W	295	103	149.2	78.4	2.9	34.7	−6.3	2.8	−19.3	212.1	2.0	115[1]	50	65.7 ± 7.4
PI6	6	62°29′30.00″N	110°42′36.00″W	21	8	11.1	−26.7	10.3	7.3	−25.1	10.3	−14.1	242.0	8.1	120[2]	55	38.3 ± 9.8
E1623A	4	62°32′20.76″N	110°33′50.40″W	104	17	337.8	−24.8	8.4	341.0	−10.8	8.4	−20.5	269.7	6.0	65[3]	0	12.0 ± 8.7
E1623B	5	62°32′56.04″N	110°42′24.84″W	51	10	321.3	−31.5	12.0	321.3	−21.5	12.0	−10.5	287.9	9.2	65[3]	0	−7.7 ± 10.4

Notes: n = number of samples, Dec = declination, Inc = inclination, α_{95} = radius of 95% confidence cone, Plat = pole latitude, Plon = pole longitude, A_{95} = radius of 95% confidence cone of the pole.
[1] structural attitude based on the measured site bedding.
[2] structural attitude based on average strike of underlying Portage Inlet Formation across a small fault; Pearson lava dips too gently for the rotation analysis.
[3] tectonically stable areas with dips too shallow for the rotation analysis; reference strike set to match trend of the McDonald Fault because of similar paleomagnetic results between Pearson Point and eastern sampling areas of McGlynn and Irving (1978).

undergone local clockwise rotations as well. Previous paleomagnetic studies of the Stark and Tochatwi Formations (Bingham and Evans, 1976; Evans and Bingham, 1976) sampled steeply-dipping (overturned) northeast-facing panels (sections BE1 and EB1 in Fig. 5; no folds in these panels) that are similar in structural attitude to Lutsel'ke Island and the mouth of Portage Inlet.

The Stark and Tochatwi Formations are stratigraphically correlated (Hoffman, 1969; Mitchell et al., 2010) with the Takiyuak Formation in the Coronation basin, where an age of 1882.5 ± 1 Ma on a tuff from the underlying Fontano Formation (Bowring and Grotzinger, 1992) constrains the maximum age of the Takiyuak Formation. Another approximately contemporaneous rock unit in the Slave craton is the 1885 Ma Ghost dykes of the Yellowknife region. Both the Takiyuak and the Ghost poles are broadly consistent with the majority of the Coronation poles (Irving and McGlynn, 1979; Buchan et al., 2016; Fig. 12). The Ghost dykes were sampled in an area where conjugate transcurrent faults are absent and the Takiyuak Formation is in a domain of dextral faults whose azimuths imply little rotation (Fig. 4b). Mitchell et al. (2010) argued that the paleocurrent azimuths of the Tochatwi Formation agree with the basin-scale structure, so that the Tochatwi pole should not be affected by local rotations. The analysis by Mitchell et al. (2010) is useful for assessing the structural corrections applied to a majority of the paleomagnetic poles obtained from the various basins marginal to Slave craton, and their model of modest (~12°) relative rotations does align well three groups of time-equivalent poles on that large spatial scale. However, the same rotations applied by Mitchell et al. (2010) are notably insufficient to align the Stark and Tochatwi poles with that of the broadly coeval Takiyuak Formation (their Fig. 6c). Assessment of the Stark and Tochatwi poles demands finer-scale analysis.

Paleocurrent data of the Tochatwi Formation (Hoffman, 1969) were collected from northwesternmost Pearson Point (section PH1 in Fig. 5) and an island in Stark Lake (section PH2 in Fig. 5), both of which have normal McDonald-parallel or sub-horizontal structural attitudes and show no evidence for paleomagnetic rotations. In fact, the Stark (site EB2 in Fig. 5) and Tochatwi (site BE2 in Fig. 5) Formations were also sampled from the island in Stark Lake, and each of them has one site with a possibly primary direction. The Stark direction agrees with the vertical-axis rotation model (Evans and Bingham, 1976), but the Tochatwi direction does not, as it might be affected by remagnetization (Bingham and Evans, 1976). Due to inadequate number of samples analyzed from areas with normal structural attitudes, the conclusion regarding whether the Stark and Tochatwi poles result from localized vertical-axis rotation in the Great Slave basin remains inconclusive. Previous Stark and Tochatwi poles need to be tested with new data from areas where structural evidence for local block rotations is absent.

The eastern end of the Coronation APWP is defined by the paleomagnetic pole from the Rifle Formation in the Kilohigok basin (Evans and Hoye, 1981; Fig. 2), subsequently dated at 1963 ± 6 Ma (Bowring and Grotzinger, 1992). Irving et al. (2004) suggest that the Rifle pole was also affected by counterclockwise rotation due to motions on the left-lateral Bathurst Fault in the Kilohigok basin. Assessing the veracity of the aberrant Rifle Formation pole requires further testing.

6. Concluding remarks

Reliable paleomagnetic poles from the Slave craton are critical in paleogeographic reconstruction of Laurentia and the supercontinent Nuna. In this study, we tested one component of the Coronation APWP, which contains multiple Slave poles between 1.96–1.87 Ga, with a detailed paleomagnetic and rock magnetic study of the ca. 1.87 Ga Pearson Formation. Results show that the magnetization of the Pearson Formation is carried by SD or small PSD magnetite grains. A positive fold test demonstrates that the Pearson remanence predates the folding of Paleoproterozoic age, supporting that magnetite grains faithfully recorded the ambient magnetic field direction during cooling after

basalt lava emplacement. Comparing the structural attitudes and paleomagnetic declinations of the Pearson Formation from different sampling areas supports the conclusion that small blocks in the Great Slave basin experienced large degrees (~60°) of vertical-axis rotation related to dextral slip on the McDonald Fault system, calling the veracity of some of the other Coronation poles into question. Further evaluation of local structural complexities indicates that the previous paleomagnetic results from the Stark and Tochatwi Formations might also be affected by vertical-axis rotation on a local scale. Although our localized result from the Pearson Formation does not preclude alternative explanations for other portions of the Coronation APWP (e.g., oscillatory true polar wander), it does confirm that paleomagnetic studies in the circum-Slave region need to be alerted to the potential for local vertical-axis rotations (Bingham and Evans, 1976; Irving et al., 2004; Mitchell et al., 2010).

Acknowledgements

We thank Sergei Pisarevsky and two anonymous reviewers for constructive comments on the manuscript. We thank Mark Brandon for discussions; Eric Bellefroid, Stephen Victor and Bin Wen for field and laboratory assistance. We thank the community of Lutsel'ke for endorsement of this study.

Appendix A. Supplementary data

Supplementary data associated with this article can be found, in the online version, at http://dx.doi.org/10.1016/j.precamres.2017.11.021.

References

Abrajevitch, A., Van der Voo, R., 2010. Incompatible Ediacaran paleomagnetic directions suggest an equatorial geomagnetic dipole hypothesis. Earth Planet. Sci. Lett. 293 (1), 164–170.
Barnes, F.Q., 1951. Snowdrift map-area. NWT. Geol. Survey Canada Paper 51–56.
Barnes, F.Q., 1953. The Snowdrift and McLean Bay map-areas, Great Slave Lake, Northwest Territories. Geology Department, University of Toronto Ph.D. thesis.
Bingham, D.K., Evans, M.E., 1976. Paleomagnetism of the Great Slave Supergroup, Northwest Territories, Canada: the Stark Formation. Can. J. Earth Sci. 13 (4), 563–578.
Bowring, S.A., 1985. U-Pb zircon geochronology of early Proterozoic Wopmay orogen, N.W.T., Canada: an example of rapid crustal evolution. University of Kansas, Lawrence Ph.D. thesis, p. 148.
Bowring, S.A., Grotzinger, J.P., 1992. Implications of new chronostratigraphy for tectonic evolution of Wopmay Orogen, Northwest Canadian Shield. Am. J. Sci. 292 (1), 1–20.
Bowring, S.A., Van Schmus, W.R., Hoffman, P.F., 1984. U-Pb zircon ages from Athapuscow aulacogen, East Arm of Great Slave Lake, N.W.T, Canada. Can. J. Earth Sci. 21, 1315–1324.
Boyden, J.A., Müller, R.D., Gurnis, M., Torsvik, T.H., Clark, J.A., Turner, M., Cannon, J.S., 2011. Next-generation plate-tectonic reconstructions using GPlates. Geoinformatics 9, 5–114.
Buchan, K.L., LeCheminant, A.N., van Breemen, O., 2009. Paleomagnetism and U-Pb geochronology of the Lac de Gras diabase dyke swarm, Slave Province, Canada: implications for relative drift of Slave and Superior provinces in the Paleoproterozoic. Can. J. Earth Sci. 46 (5), 361–379.
Buchan, K.L., Ernst, R.E., Bleeker, W., Davis, W.J., Villeneuve, M., van Breemen, O., Hamilton, M.A., Söderlund, U., 2010. Proterozoic Magmatic Events of the Slave Craton, Wopmay Orogen and Environs. Geological Survey of Canada, Open File 5989, CD-ROM, poster and 25 pp. report.
Buchan, K.L., Mitchell, R.N., Bleeker, W., Hamilton, M.A., LeCheminant, A.N., 2016. Paleomagnetism of ca. 2.13-2.11 Ga Indin and ca. 1.885 Ga Ghost dyke swarms of the Slave craton: Implications for the Slave craton APW path and relative drift of Slave, Superior and Siberian cratons in the Paleoproterozoic. Precambr. Res. 275, 151–175.
Butler, R.F., 1992. Paleomagnetism: Magnetic Domains to Geologic Terranes. Blackwell Scientific p. 238.
Cardozo, N., Allmendinger, R.W., 2013. Spherical projections with OSXStereonet. Comput. Geosci. 51, 193–205.
Carey, S.W., 1958. The tectonic approach to continental drift. In: Carey, S.W. (Ed.), Continental Drift: A Symposium. Geology Department, University of Tasmania, Hobart, pp. 177–355.
Cloos, E., 1955. Experimental analysis of fracture patterns. Geol. Soc. Am. Bull. 66, 241–256.
Cook, F.A., 2011. Multiple arc development in the Palaeoproterozoic Wopmay orogen, northwest Canada. In: Brown, D., Ryan, P.D. (Eds.), Arc-Continent Collision. Springer-Verlag, Heidelberg, pp. 403–427.
Cox, A., Doell, R.R., 1964. Long period variations of the geomagnetic field. Bull. Seismol. Soc. Am. 54 (6B), 2243–2270.
Creveling, J.R., Mitrovica, J.X., Chan, N.H., Latychev, K., Matsuyama, I., 2012. Mechanisms for oscillatory true polar wander. Nature 491 (7423), 244.
Davis, W.J., Bleeker, W., Hulbert, L., Jackson, V., 2004. New geochronological results from the Slave Province Minerals and Geoscience Compilation and Synthesis Project. In Geological Science of Canada Northern Resources Program: Yellowknife Geoscience Forum (Abstracts of Talks and Posters), p. 20.
Day, R., Fuller, M., Schmidt, V.A., 1977. Hysteresis properties of titanomagnetites: grain-size and compositional dependence. Phys. Earth Planet. Inter. 13 (4), 260–267.
Dunlop, D.J., 2002. Theory and application of the Day plot (Mrs/Ms versus Hcr/Hc) 1. Theoretical curves and tests using titanomagnetite data. J. Geophys. Res.: Solid Earth 107 (B3).
Enkin, R.J., 2003. The direction-correction tilt test: an all-purpose tilt/fold test for paleomagnetic studies. Earth Planet. Sci. Lett. 212, 151–166.
Evans, D.A., 1998. True polar wander, a supercontinental legacy. Earth Planet. Sci. Lett. 157 (1–2), 1–8.
Evans, M.E., Hoye, G.S., Bingham, D.K., 1980. The paleomagnetism of the Great Slave supergroup: the Akaitcho River formation. Can. J. Earth Sci. 17 (10), 1389–1395.
Evans, M.E., Bingham, D.K., 1976. Paleomagnetism of the Great Slave Supergroup, Northwest Territories, Canada: the Tochatwi Formation. Can. J. Earth Sci. 13 (4), 555–562.
Evans, M.E., Hoye, G.S., 1981. Paleomagnetic Results from the Lower Proterozoic Rocks of Great Slave Lake and Bathurst Inlet Areas, Northwest Territories. Proterozoic Basins of Canada: Geological Survey of Canada Paper pp. 81–10.
Freund, R., 1970. Rotation of strike-slip faults in Sistan, southeast Iran. J. Geol. 78, 188–200.
Freund, R., 1974. Kinematics of transform and transcurrent faults. Tectonophysics 21, 93–134.
Gibb, R.A., 1978. Slave-Churchill collision tectonics. Nature 271, 50–52.
Gold, T., 1955. Instability of the Earth's axis of rotation. Nature 175 (4456), 526–529.
Halls, H.C., Lovette, A., Hamilton, M., Söderlund, U., 2015. A paleomagnetic and U-Pb geochronology study of the western end of the Grenville dyke swarm: Rapid changes in paleomagnetic field direction at ca. 585 Ma related to polarity reversals? Precambr. Res. 257, 137–166.
Helmstaedt, H., 2009. Crust-mantle coupling revisited: the Archean Slave craton, NWT, Canada. Lithos 112, 1055–1068.
Hildebrand, R.S. Geology, Rainy Lake-White Eagle Falls area, District of Mackenzie. Geological Survey of Canada, Map 1546A, 1: 50,000 scale map, 1985.
Hildebrand, R.S., 1987. Tectono-magmatic evolution of the 1.9-Ga Great Bear magmatic zone, Wopmay orogen, northwestern Canada. J. Volcanol. Geoth. Res. 32, 99–118.
Hildebrand, R.S., Hoffman, P.F., Housh, T., Bowring, S.A., 2010. The nature of volcano-plutonic relations and the shapes of epizonal plutons of continental arcs as revealed in the Great Bear magmatic zone, northwestern Canada. Geosphere 6, 1–28.
Hildebrand, R.S. Geological synthesis: northern Wopmay orogen/Coppermine homocline, Northwest Territories-Nunavut. Geological Survey of Canada, Open File 6390, 1: 500, 000 scale map, 2011.
Hoffman, K.A., 1991. Long-lived transitional states of the geomagnetic field and the two dynamo families. Nature 354 (6351), 273–277.
Hoffman, P.F., 1968. Stratigraphy of the lower Proterozoic (Aphebian), Great Slave Supergroup, east arm of Great Slave Lake, District of Mackenzie. Geological Survey of Canada Paper 68-42, p. 93.
Hoffman, P., 1969. Proterozoic paleocurrents and depositional history of the East Arm fold belt, Great Slave Lake, Northwest Territories. Can. J. Earth Sci. 6 (3), 441–462.
Hoffman, P., 1973. Evolution of an early Proterozoic continental margin: the Coronation geosyncline and associated aulacogens of the northwestern Canadian shield. Philos. Trans. Royal Soc. London A: Math., Phys. Eng. Sci. 273 (1235), 547–581.
Hoffman, P.F., Bell, I.R., Hildebrand, R.S., Thorstad, L., 1977. Geology of the Athapuscow Aulacogen, East Arm of Great Slave Lake, District of Mackenzie. In Report of Activities. Part A, Geological Survey of Canada Paper 77-1A, 117–129.
Hoffman, P.F., 1980. Wopmay orogen: a Wilson cycle of Early Proterozoic age in the northwest of the Canadian Shield. In: The Continental Crust and Its Mineral Resources, Geological Association of Canada. In: Strangway, D.W. (Ed.), 20. Special Publication, pp. 523–549.
Hoffman, P.F., 1981. Autopsy of Athapuscow Aulacogen: a failed arm affected by three collisions. In Campbel, F. H. A., ed. Proterozoic Basins of Canada. Geol. Surv. Can. Pap. 81–10, 97–102.
Hoffman, P.F., 1988a. United plates of America, the birth of a craton: early Proterozoic assembly and growth of Laurentia. Annu. Rev. Earth Planet. Sci. 16 (1), 543–603.
Hoffman, P.F., Geology and tectonics, East Arm of Great Slave Lake, Northwest Territories. Geological Survey of Canada, Map 1628A, scale 1: 250,000 and 1: 500, 000, 1988.
Hoffman, P.F., 1989. Precambrian geology and tectonic history of North America. Geol. North Am. 447–512.
Hoffman, P.F., Geology, northern externides of Wopmay orogen, District of Mackenzie. Geological Survey of Canada, Open File 3251, 1: 250,000-scale map, 1994.
Hoffman, P.F., 2014. The origin of Laurentia: Rae craton as the backstop for proto-Laurentian amalgamation by slab suction. Geosci. Can. 41, 313–320.
Hornafius, J.S., Luyendyk, B.P., Terres, R.R., Kamerling, M.J., 1986. Timing and extent of Neogene tectonic rotation in the western Transverse Ranges, California. Geol. Soc. Am. Bullet. 97 (12), 1476–1487.
Irving, E., Park, J.K., McGlynn, J.C., 1972. Paleomagnetism of the Et-Then Group and Mackenzie Diabase in the Great Slave Lake Area. Can. J. Earth Sci. 9, 744–755.
Irving, E., McGlynn, J.C., 1979. Palaeomagnetism in the Coronation Geosyncline and arrangement of continents in the middle Proterozoic. Geophys. J. Int. 58 (2), 309–336.
Irving, E., Baker, J., Hamilton, M., Wynne, P.J., 2004. Early Proterozoic geomagnetic field

in western Laurentia: implications for paleolatitudes, local rotations and stratigraphy. Precambr. Res. 129 (3), 251–270.
Jones, C.H., 2002. User-driven integrated software lives: “Paleomag” paleomagnetics analysis on the Macintosh. Comput. Geosci. 28 (10), 1145–1151.
Kamerling, M.J., Luyendyk, B.P., 1979. Tectonic rotations of the Santa Monica Mountains region, western Transverse Ranges, California, suggested by paleomagnetic vectors. Geol. Soc. Am. Bullet. 90 (4), 331–337.
Kilian, T.M., Chamberlain, K.R., Evans, D.A., Bleeker, W., Cousens, B.L., 2016. Wyoming on the run-Toward final Paleoproterozoic assembly of Laurentia. Geology 44 (10), 863–866.
Kim, Y.S., Peacock, D.C.P., Sanderson, D.J., 2004. Fault damage zones. J. Struct. Geol. 26, 503–517.
Kirschvink, J.L., 1980. The least-squares line and plane and the analysis of palaeomagnetic data. Geophys. J. Int. 62 (3), 699–718.
Kirschvink, J.L., Kopp, R.E., Raub, T.D., Baumgartner, C.T., Holt, J.W., 2008. Rapid, precise, and high-sensitivity acquisition of paleomagnetic and rock-magnetic data: Development of a low-noise automatic sample changing system for superconducting rock magnetometers. Geochem. Geophys. Geosyst. 9 (5).
Lowell, J.D., 1972. Spitsbergen tertiary orogenic belt and the spitsbergen fracture zone. Geol. Soc. Am. Bull. 83, 3091–3102.
McGlynn, J.C., Irving, E., 1978. Multicomponent magnetization of the Pearson Formation (Great Slave Supergroup, NWT) and the Coronation loop. Can. J. Earth Sci. 15 (4), 642–654.
Mitchell, R.N., Hoffman, P.F., Evans, D.A., 2010. Coronation loop resurrected: oscillatory apparent polar wander of Orosirian (2.05-1.8 Ga) paleomagnetic poles from Slave craton. Precambr. Res. 179 (1), 121–134.
Mitchell, R.N., Bleeker, W., Van Breemen, O., LeCheminant, T.N., Peng, P., Nilsson, M.K., Evans, D.A., 2014. Plate tectonics before 2.0 Ga: Evidence from paleomagnetism of cratons within supercontinent Nuna. Am. J. Sci. 314 (4), 878–894.
Muxworthy, A.R., McClelland, E., 2000. Review of the low-temperature magnetic properties of magnetite from a rock magnetic perspective. Geophys. J. Int. 140 (1), 101–114.
Raub, T.D., Kirschvink, J.L., Evans, D.A.D., 2007. True polar wander: linking deep and shallow geodynamics to hydro-and biospheric hypotheses. Treat. Geophys. 5, 565–589.
Reid, A.B., McMurry, E.W., Evans, M.E., 1981. Paleomagnetism of the Great Slave Supergroup, Northwest Territories, Canada: multicomponent magnetization of the Kahochella Group. Can. J. Earth Sci. 18 (3), 574–583.
Ritts, B.D., Grotzinger, J.P., 1994. Depositional facies and detrital composition of the Paleoproterozoic Et-then Group, N.W.T., Canada: sedimentary response to intracratonic indentation. Can. J. Earth Sci. 31, 1763–1778.
Rose, I., Buffett, B., 2017. Scaling rates of true polar wander in convecting planets and moons. Phys. Earth Planet. Inter. 273, 1–10.
Segall, P., Pollard, D.D., 1980. Mechanics of discontinuous faults. J. Geophys. Res. 85 (B8), 4337–4350.
Spada, G., Ricard, Y., Sabadini, R., 1992. Excitation of true polar wander by subduction. Nature 360 (6403), 452–454.
Steinberger, B., Seidel, M.L., Torsvik, T.H., 2017. Limited true polar wander as evidence that Earth's nonhydrostatic shape is persistently triaxial. Geophys. Res. Lett. 44 (2), 827–834.
Stockwell, C. H., Great Slave Lake-Coppermine River area, Northwest Territories, Geological Survey of Canada, Annual Reports, Part C, pp. 37-63, 1932.
Stockwell, C.H., Eastern portion of Great Slave Lake, District of Mackenzie, Northwest Territories. Geological Survey of Canada, Maps 377A and 378A (with descriptive notes), 1936.
Tirrul, R., Geology and structural restoration of the east-central part of Asiak thrust-fold belt, Wopmay orogen, Northwest Territories. Geological Survey of Canada, Map 1654A, 2 sheets, 1: 50,000 scale, 1992.
Tauxe, L., 1998. Paleomagnetic Principles and Practice. Kluwer Academic Publishers, Modern approaches in geophysics.
Thomas, M.D., Gibb, R.A., Quince, J.R., 1976. New evidence from offset aeromagnetic anomalies for transcurrent faulting associated with the Bathurst and McDonald faults, Northwest Territories. Can. J. Earth Sci. 13, 1244–1250.
Tsai, V.C., Stevenson, D.J., 2007. Theoretical constraints on true polar wander. J. Geophys. Res. Solid Earth 112 (B5).
Verosub, K.L., 1988. Geomagnetic secular variation and the dating of Quaternary sediments. Geol. Soc. Am. Spec. Papers 227, 123–138.
Wilcox, R.E., Harding, T.P., Seely, D.R., 1973. Basic wrench tectonics. Am. Assoc. Pet. Geol. Bull. 57, 74–96.
Zijderveld, J.D.A., 1967. AC demagnetization of rocks: analysis of results. Methods paleomagnetism 3, 254.